Volume 1 | Number 1 | Jan 2013 | Pages 1–100

Journal of
Materials Chemistry A

Materials for energy and sustainability
www.rsc.org/materialsA

Li⁺

ROYAL SOCIETY
OF CHEMISTRY

ROYAL SOCIETY
OF CHEMISTRY

www.rsc.org/materialsA

Journal of Materials Chemistry A

COMMUNICATION

A quantum dot and iron sulphur electrocatalyst sensitized porous silicon photocathode

Soundarrajan Chandrasekaran [a†], Thomas J. Macdonald [b†], Yatin J. Mange [b], Nicolas H. Voelcker *[a] and Thomas Nann *[b]

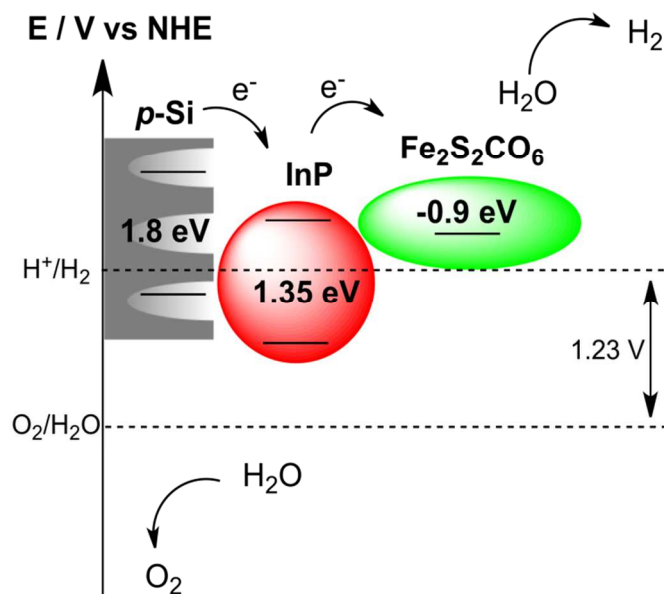**Solar fuels have attracted considerable attention as an alternative energy vector in the context of the dwindling supplies of the planet's non-renewable resources. The first step in solar fuel generation is often a photo-catalytic water-splitting. Although a very large amount of work has been dedicated to optimise the photo-oxidation process (mostly based on titania), the development of highly efficient photocathodes is limited. In this paper, we report on the fabrication and characterisation of a nano-structured photocathode using indium phosphide QDs and a bio-inspired $Fe_2S_2(CO)_6$ catalyst sensitized on a p-type porous silicon electrode. Our hybrid electrode system produced a photocurrent density of -1.2 mA/cm^2 with hydrogen evolution at low bias potentials.**

Diminishing fossil fuel vectors and increasing carbon dioxide levels in the atmosphere are major drivers for research into renewable energy sources. In artificial photosynthesis, solar energy is converted into chemical energy by following the blueprint of natural photosynthesis. This is attractive because it allows for the storage of the fuel and thus offers a solution to intermittent energy supply. Research on artificial photosynthesis is characterised by a diversity of approaches, for example supramolecular structures[1], inorganic[2] and hybrid devices[3]. A typical artificial photosynthesis device consists of a photoanode, where oxidation occurs, and a reducing photocathode. Both photoelectrodes contain a pigment mimicking chlorophyll and a catalyst, analogous to the natural enzyme cascades. In inorganic systems, the photoanode is usually based on an *n-type* semiconductor such as titanium dioxide (TiO_2), whilst the photocathode is based on a *p-type* semiconductor. As catalysts, molecular[4] or heterogeneous catalysts[5] have been employed. *p-type* silicon has been previously recognised as a promising photoactive cathode material for artificial photosynthesis[6-10]. This is attributable to a low band gap of 1.12 eV, which allows for the absorption of a large fraction of the visible spectrum when compared to photoelectrode materials such as TiO_2 (band gap 3.2 eV) or gallium phosphide (GaP: band gap 2.2 eV). Furthermore, the position of the conduction band of silicon is well aligned with the reduction potential of protons. Porous silicon (pSi) produced as a result of electrochemical etching has a band gap of between 1.8-2.2 eV[11, 12]. Other salient features exemplifying the potential of the material in

this field include element abundance in the earth's crust, high solar energy conversion efficiency, broad solar absorption spectrum and successful track record as starting material for other industrial electrical and electronic applications[13]. Recently, Oh *et al.*, investigated the photocurrent efficiency of pSi and found that platinum (Pt) impregnation by electroless deposition reduced the overpotential for photoelectrochemical hydrogen generation[14]. More recently, Ott *et al.*,[15] fabricated a *p-type* silicon/molecular electro-catalyst junction using a dithiolate-bridged [FeFe] motif, a derivative of the $Fe_2S_2(CO)_6$ hydrogenase analogue used in our earlier work[2]. In this study, we aimed to increase the efficiency of the solar-driven hydrogen generation by harnessing the properties of pSi in combination with [FeFe] hydrogenase analogues as electrocatalysts. We focus on assembling a hierarchically nanostructured photocathode from *p-type* pSi, indium phosphide (InP) semiconductor quantum dots (QDs) and $Fe_2S_2(CO)_6$ catalyst (Scheme 1).

Scheme 1. Schematic representation of the band gap energy of InP QDs and

This journal is © The Royal Society of Chemistry 2014

J. Mater. Chem. A, 2014, **00**, 1-3 | **1**

$Fe_2S_2(CO)_6$ catalyst attached inside *p-type* pSi as well as charge transfers leading to electrochemical reduction of protons to hydrogen.

Fourier transform infrared spectrum (FTIR) of the carbonyl stretching region of $Fe_2S_2(CO)_6$ catalyst in toluene is shown in Figure S1. This particular catalyst was chosen since it has been previously shown to bind efficiently to InP QDs and catalyses the electrochemical reduction of protons to dihydrogen[2]. Our strategy resulted in a photocathode with superior performance yielding an applied bias photo-to-current efficiency (ABPE) of 0.63% while evolving hydrogen gas[16]. *p-type* silicon (resistivity 0.5-1mΩ cm) was anodised to form uniform pores of approximately 50 nm diameter and pore depths of 13.2 μm, as is evident from top-view and cross-sectional scanning electron microscopy (SEM) images (Figure 1 A and C). Since we found that the formation of an insulating oxide layer on the pSi surface was detrimental to the long-term performance of the photocathode, the freshly etched, hydride-terminated pSi was capped with a methyl layer by electrografting[17, 18] to protect the surface from oxidation (Figure S2). InP QDs were synthesized following a procedure similar to that by Reiss *et al.*[19] (see supporting information). This resulted in QDs of 5-9 nm diameter (confirmed by transmission electron microscopy (TEM) and dynamic light scattering (DLS) - Figure S3) bearing non-polar octadecene ligands on their surface. The photoluminescence of the QDs had an emission maximum at 610 nm and a full width at half maximum (FWHM) of ~200 nm (Figure S3).
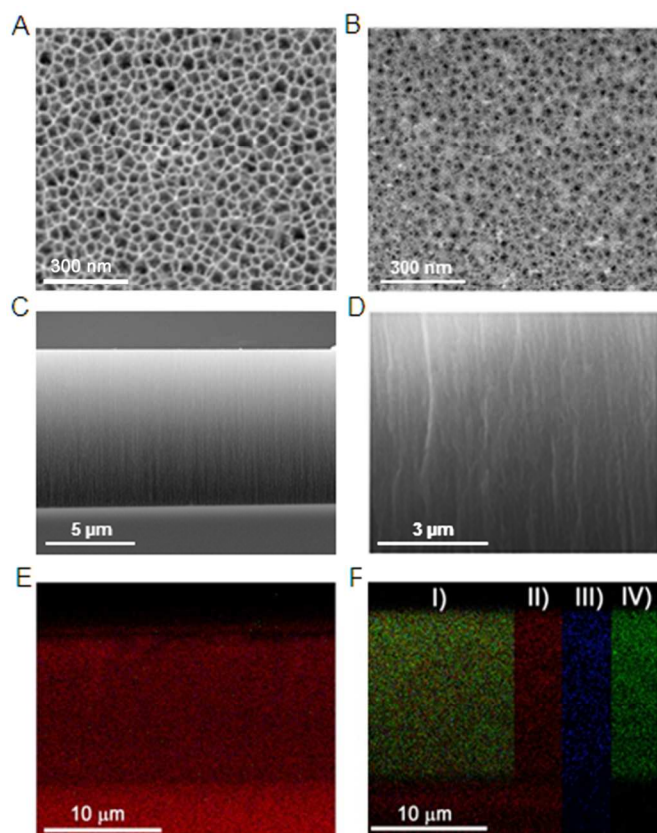

Figure 1: A and B show the SEM top-view images of bare pSi and pSi loaded with QDs and catalyst. C and D show the corresponding cross-sectional SEM images. E and F show the corresponding cross-sectional ToF-SIMS ion maps (red, green, and blue representing Si+, In+ and Fe+). Image F shows also individual colour channels for clarity, where I) merged, II)-IV) Si, Fe and In signals, respectively.

Given that the diameter of the QDs was adequate for ingress into the pores of the pSi (size ratio QD/pSi pores 5:1)[20], we then assembled the photocathode by subsequent physisorption of the QDs and $Fe_2S_2(CO)_6$ catalyst molecules. Figure 1 B and D show the top-view and cross-sectional SEM images after loading the pSi with QDs and catalyst. The average pore size decreased from ∼ 50 nm to ∼ 35 nm, suggesting that the QDs have indeed adsorbed onto the walls of the pSi pores. In addition, the presence of both indium and iron moieties inside the pSi, indicative of InP QDs and $Fe_2S_2(CO)_6$ catalyst, respectively, was confirmed by means of energy-dispersive X-ray spectroscopy (EDXS) (Figure S4). Figure 1 E and F show the cross sectional images of time-of-flight secondary ion mass spectrometry (ToF-SIMS) of bare pSi and pSi loaded with QDs and $Fe_2S_2(CO)_6$. The red, green and blue colours correspond to Si (m/z 28), In (115 m/z) and Fe (55 m/z) ions, respectively. In and Fe ion signals are found throughout the porous layer in the loaded sample, but are absent in the unloaded sample, demonstrating that the QDs and catalyst penetrated all the way to the pSi-bulk Si interface. The mass spectra in Figure S5 also confirm the presence of In and Fe moieties inside the pSi layer near the pSi/Si interface. Figure 2 shows the increase in photocurrent density by ramping up the bias potential in steps of -100 mV for electrografted pSi loaded with InP and $Fe_2S_2(CO)_6$ catalyst vs. Ag|AgCl in 0.1M H_2SO_4 as electrolyte. The inset shows the photocurrent density measured using the assembled photocathode at a bias potential of -500 mV over two light-dark cycles. It showed a photocurrent density of $-1.2mA/cm^2$ with a significant amount of hydrogen bubbles produced. The hydrogen bubbles were analysed using gas chromatography (Figure S6). Figure S7 shows the performance of the assembled photocathode over 50 minutes with 10 minutes light-dark cycles at a bias potential of -500 mV. This indicates that the assembled photocathode is capable of producing hydrogen for longer cycles. In all experiments, cell was irradiated with a calibrated light intensity of 100 mW/cm^2 under air mass (AM) 1.5 conditions.
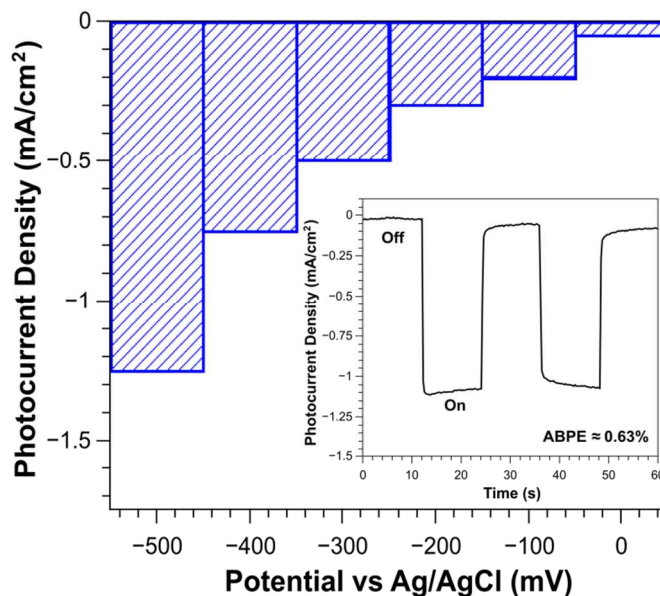

Figure 2: The increase in photocurrent density with increasing bias potentials in steps of -100 mV for electrografted pSi loaded with InP and $Fe_2S_2(CO)_6$ catalyst. The inset shows two light-dark photocurrent cycles measured at a bias potential of -500 mV.

Figure 3 shows the effect of methyl-capping and also the effect of loading pSi with either InP QDs or $Fe_2S_2(CO)_6$ catalyst only at a bias potential of -500 mV. In most cases, the electrografted pSi nearly

doubled the photocurrent efficiency. In addition, photocathodes with non-electrografted pSi rapidly declined in photoelectrochemical performance. We note that hydrosilylation of octene or undecene also protected the pSi surface but resulted in small photocurrent density, confirming that methyl electrografting is a superior surface functionalisation technique for pSi photoelectrochemistry. InP QDs loading alone did not improve the photocurrent density over bare pSi. Indeed, the measured photocurrent density decreased slightly. This may be due to the hindrance of the surface ligands of the InP quantum dots in electron conduction. Addition of the catalyst in the absence of the InP QDs resulted in a photocurrent density of -0.4 mA/cm^2. A significant increase in the photocurrent density of -1.2 mA/cm^2 was observed for the electrografted pSi containing both InP QDs and $Fe_2S_2(CO)_6$ catalyst.
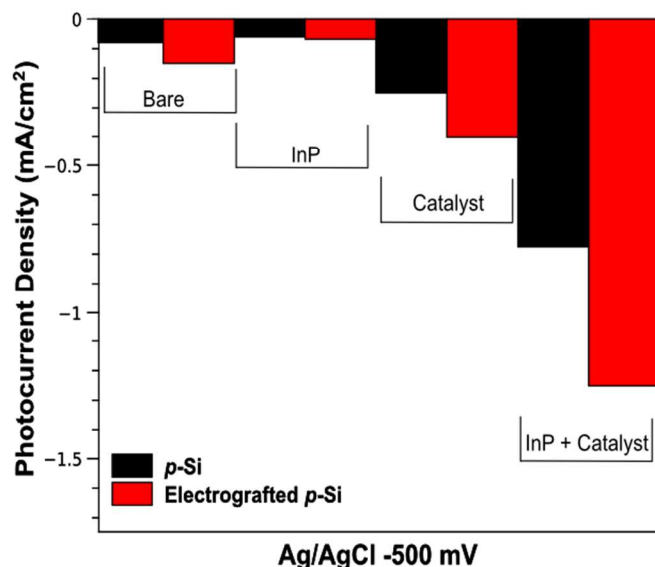

Figure 3: The effect of electrografting on the photocurrent density before and after loading pSi with InP QDs and $Fe_2S_2(CO)_6$ catalyst at a bias potential of -500 mV versus Ag/AgCl in 0.1M H_2SO_4.

The ABPE of the photocathode was evaluated in a three-electrode cell assembly. The ABPE was calculated as follows[6]:

$$ABPE = \left[\frac{j \,(mA\,cm^{-2}) \times (1.23V - Vb)}{Pi \,(mW\,cm^{-2})} \right] \times 100\%$$

in which j (mA cm^{-2}) is the measured photocurrent density, V_b is the bias between the working electrode, counter electrode and reference electrode calculated vs NHE, and P_i is the incident light intensity (100 mW cm^{-2}).

Our photocathode system facilitated the conversion of photons of light into electrical power with an ABPE = 0.63% for the reduction of protons to hydrogen. Comparing our results with those of Ott *et al.* [15], we recognize that their photocurrent density was higher compared to ours. However, our system showed the electrode surface was protected from oxidation and demonstrably produced hydrogen. Efforts to further improve the efficiency of our photocathode by tailoring the pSi properties are currently under way.

Conclusions

In conclusion, we report here the first example of sensitizing a pSi electrode to produce hydrogen in an aqueous electrolyte using a combination of InP QDs and $Fe_2S_2(CO)_6$ catalyst. With the ABPE efficiency of 0.63%, our hybrid system showed 90% improvement in photocurrent density when compared to bare pSi. While other *p-type* photocathodes have been produced, this is the first device, which utilizes the surface area provided by the pores in *p-type* silicon. Thus we developed a three dimensional nanostructured photocathode for hydrogen production.

ACKNOWLEDGMENT

Notes and references

[a] Mawson Institute, University of South Australia, Mawson Lakes Blvd, Adelaide, SA 5095, Australia.

[b] Ian Wark Research Institute, University of South Australia, Mawson Lakes Blvd, Adelaide, SA 5095, Australia.

† Soundarrajan Chandrasekaran and Thomas J. Macdonald contributed equally to this publication

Electronic Supplementary Information (ESI) available: Detailed experimental materials and methods, InP synthesis procedure and supplementary figures. See DOI: 10.1039/c000000x/

1. M. R. Wasielewski, *Chemical Reviews*, 1992, **92**, 435-461.
2. T. Nann, S. K. Ibrahim, P.-M. Woi, S. Xu, J. Ziegler and C. J. Pickett, *Angewandte Chemie International Edition*, 2010, **49**, 1574-1577.
3. M. Quintana, A. M. López, S. Rapino, F. M. Toma, M. Iurlo, M. Carraro, A. Sartorel, C. Maccato, X. Ke, C. Bittencourt, T. Da Ros, G. Van Tendeloo, M. Marcaccio, F. Paolucci, M. Prato and M. Bonchio, *ACS Nano*, 2012, **7**, 811-817.
4. K. S. Joya, J. L. Vallés-Pardo, Y. F. Joya, T. Eisenmayer, B. Thomas, F. Buda and H. J. M. de Groot, *ChemPlusChem*, 2013, **78**, 35-47.
5. A. Kudo and Y. Miseki, *Chemical Society Reviews*, 2009, **38**, 253-278.
6. R. N. Dominey, N. S. Lewis, J. A. Bruce, D. C. Bookbinder and M. S. Wrighton, *Journal of the American Chemical Society*, 1982, **104**, 467-482.
7. J. Oh, T. G. Deutsch, H.-C. Yuan and H. M. Branz, *Energy & Environmental Science*, 2011, **4**, 1690-1694.

8. S. W. Boettcher, E. L. Warren, M. C. Putnam, E. A. Santori, D. Turner-Evans, M. D. Kelzenberg, M. G. Walter, J. R. McKone, B. S. Brunschwig, H. A. Atwater and N. S. Lewis, *Journal of the American Chemical Society*, 2011, **133**, 1216-1219.

9. Y. Hou, B. L. Abrams, P. C. K. Vesborg, M. E. Björketun, K. Herbst, L. Bech, A. M. Setti, C. D. Damsgaard, T. Pedersen, O. Hansen, J. Rossmeisl, S. Dahl, J. K. Nørskov and I. Chorkendorff, *Nat Mater*, 2011, **10**, 434-438.

10. J. A. Bruce and M. S. Wrighton, *Israel Journal of Chemistry*, 1982, **22**, 184-189.

11. J. T. Frederiksen, P. G. Melcher and E. Veje, *Journal of Porous Materials*, 2000, **7**, 271-273.

12. Z. Chen, T. Lee, x, Yin and G. Bosman, *Applied Physics Letters*, 1994, **64**, 3446-3448.

13. K. Sun, K. Madsen, P. Andersen, aring, W. Bao, Z. Sun and D. Wang, *Nanotechnology*, 2012, **23**, 194013.

14. I.-W. K. Oh, Joo-Hong ; Hwang, Seong-Pil *Bulletin of the Korean Chemical Society*, 2011, **32**, 4392-4396.

15. B. Kumar, M. Beyler, C. P. Kubiak and S. Ott, *Chemistry – A European Journal*, 2012, **18**, 1295-1298.

16. K. Zhang, D. Jing, C. Xing and L. Guo, *International Journal of Hydrogen Energy*, 2007, **32**, 4685-4691.

17. I. N. Lees, H. Lin, C. A. Canaria, C. Gurtner, M. J. Sailor and G. M. Miskelly, *Langmuir*, 2003, **19**, 9812-9817.

18. D. Belanger and J. Pinson, *Chemical Society Reviews*, 2011, **40**, 3995-4048.

19. L. Li, M. Protière and P. Reiss, *Chemistry of Materials*, 2008, **20**, 2621-2623.

20. K. Rumpf, P. Granitzer, P. Morales, P. Poelt and M. Reissner, *Nanoscale Research Letters*, 2012, **7**, 445.

Journal of Materials Chemistry A Accepted Manuscript